

## Video Article

# A Portal Vein Injection Model to Study Liver Metastasis of Breast Cancer

Erica T. Goddard<sup>1</sup>, Jacob Fischer<sup>1</sup>, Pepper Schedin<sup>1</sup><sup>1</sup>Department of Cell, Developmental and Cancer Biology, Oregon Health and Science UniversityCorrespondence to: Pepper Schedin at [schedin@ohsu.edu](mailto:schedin@ohsu.edu)URL: <http://www.jove.com/video/54903>DOI: [doi:10.3791/54903](https://doi.org/10.3791/54903)

Keywords: Cancer Research, Issue 118, liver metastasis, portal vein, intraportal injection, breast cancer, survival surgery, mouse model

Date Published: 12/26/2016

Citation: Goddard, E.T., Fischer, J., Schedin, P. A Portal Vein Injection Model to Study Liver Metastasis of Breast Cancer. *J. Vis. Exp.* (118), e54903, doi:10.3791/54903 (2016).

## Abstract

Breast cancer is the leading cause of cancer-related mortality in women worldwide. Liver metastasis is involved in upwards of 30% of cases with breast cancer metastasis, and results in poor outcomes with median survival rates of only 4.8 - 15 months. Current rodent models of breast cancer metastasis, including primary tumor cell xenograft and spontaneous tumor models, rarely metastasize to the liver. Intracardiac and intrasplenic injection models do result in liver metastases, however these models can be confounded by concomitant secondary-site metastasis, or by compromised immunity due to removal of the spleen to avoid tumor growth at the injection site. To address the need for improved liver metastasis models, a murine portal vein injection method that delivers tumor cells firstly and directly to the liver was developed. This model delivers tumor cells to the liver without complications of concurrent metastases in other organs or removal of the spleen. The optimized portal vein protocol employs small injection volumes of 5 - 10  $\mu$ l,  $\geq$  32 gauge needles, and hemostatic gauze at the injection site to control for blood loss. The portal vein injection approach in Balb/c female mice using three syngeneic mammary tumor lines of varying metastatic potential was tested; high-metastatic 4T1 cells, moderate-metastatic D2A1 cells, and low-metastatic D2.OR cells. Concentrations of  $\leq$  10,000 cells/injection results in a latency of ~ 20 - 40 days for development of liver metastases with the higher metastatic 4T1 and D2A1 lines, and > 55 days for the less aggressive D2.OR line. This model represents an important tool to study breast cancer metastasis to the liver, and may be applicable to other cancers that frequently metastasize to the liver including colorectal and pancreatic adenocarcinomas.

## Video Link

The video component of this article can be found at <http://www.jove.com/video/54903/>

## Introduction

### Breast Cancer Metastasis to the Liver

The liver is a common site of breast cancer metastasis, along with bone and lung<sup>1-3</sup>. Liver metastasis in breast cancer patients is an independent prognostic factor for very poor outcomes<sup>4,5</sup>, as median survival of breast cancer patients with liver metastasis ranges from 4.8 to 15 months<sup>6-9</sup>. In contrast, breast cancer patients with lung or bone metastasis have median survival rates of 9 to 27.4 months<sup>8,9</sup> and 16.3 to 56 months<sup>8,10-12</sup>, respectively. Metastasis is a multistep process, referred to as the metastatic cascade, which begins with tumor cell dissemination in the primary tumor and ends with patient mortality due to the seeding and outgrowth of circulating tumor cells within a distant organ<sup>13-15</sup>. Rodent models of metastasis have revealed that the metastatic cascade is remarkably inefficient, with only 0.02 - 10% of circulating tumor cells establishing overt metastasis<sup>16,17</sup>. One major bottleneck of metastatic inefficiency is dictated by the unique tissue microenvironments at secondary sites, called metastatic niches<sup>18</sup>, highlighting the importance of understanding site-specific metastasis. The metastatic niche is unique to the site of recurrence, and is, in part, characterized by deposition of distinct extracellular matrix proteins<sup>19,20</sup>, infiltration of various immune cell populations<sup>21-23</sup>, and altered tissue homeostasis including dysregulated production of numerous cytokines, chemokines, and growth factors<sup>15,18,24,25</sup>. Thus, an understanding of the tissue specific metastatic niche precedes an understanding of how to target metastatic disease. However, robust models of liver metastasis are lacking. Further, improved models of liver metastasis will be essential to identifying novel targets and effective treatments for breast cancer patients with liver metastases.

### Established Models to Study Breast Cancer Metastasis to the Liver

Currently available models to study breast cancer metastasis to the liver include human cancer cell xenografts in immune compromised mice. These models typically use well-studied human breast cancer cell lines such as MCF-7 and MDA-MB-231 and Nude, Rag1<sup>-/-</sup>, or SCID immune compromised murine hosts<sup>26-29</sup>. Xenograft models provide the advantage of involving human derived cancer cell lines, however, given the recent appreciation for immune cells in metastasis<sup>30-32</sup> and in therapeutic resistance<sup>33-35</sup>, the study of metastasis in a fully immune competent host is paramount. Models to study breast cancer metastasis to the liver in immune competent hosts include orthotopic injection of syngeneic tumor cells (e.g., 4T1 and D2A1 cell lines) into the mammary fat pad, with or without surgical resection of the primary tumor, and subsequent assessment of metastasis<sup>36-38</sup>. Of note, the rate of liver metastasis from orthotopic transplant models is very low or non-existent compared to other metastatic sites such as lung<sup>39,40</sup>, or occurs after lung metastasis is established, complicating the study of liver-specific metastasis<sup>37,39</sup>.

Tumor explants from spontaneous genetically engineered breast cancer models can be re-injected into the mammary fat pads of naïve hosts as syngeneic tumor cells. For example, it was recently reported that spontaneous tumors from K14<sup>Cre</sup>ECad<sup>fl/fl</sup>P53<sup>fl/fl</sup> mice, which model invasive lobular breast carcinoma, develop tumors when orthotopically injected into wildtype hosts. Following surgical resection of these tumors once they reach 15 mm<sup>2</sup>, 18% of the mice progressed to liver metastasis<sup>40,41</sup>. A third approach to model liver metastasis utilizes spontaneous metastasis in genetically engineered mice. To date, reports of spontaneous murine models of breast cancer metastasis that readily spread to the liver are uncommon. Exceptions include the H19-IGF2, the p53<sup>tp/tp</sup> MMTV-Cre Wap-Cre, and the K14<sup>Cre</sup>ECad<sup>fl/fl</sup>P53<sup>fl/fl</sup> genetically engineered mouse models, where liver metastasis develops in a low percentage of mice<sup>38,41-43</sup>. Thus, while genetically engineered mouse models facilitate the study of all stages of the metastatic cascade, providing powerful and clinically relevant models, they are limited due to low rates of liver metastasis<sup>38</sup>.

Several metastasis models bypass the initial steps of the metastatic cascade including dissemination of tumor cells from the primary tumor and intravasation. These models permit investigation into the later steps of the metastatic cascade, from extravasation to establishment of tumors at secondary sites. The intracardiac injection model delivers tumor cells into the left ventricle, which distributes tumor cells into the circulatory system via the aorta. Intracardiac injection requires ultrasound guided imaging of the injection site or other imaging modalities such as bioluminescence of luciferase tagged cells to confirm successful injection. Tumor cell injection via the left ventricle may result in bone, brain, lung, and/or liver metastasis, amongst other organs<sup>44-48</sup>. Because of multi-organ metastases, these mice frequently need to be euthanized prior to development of overt liver metastasis, negating the ability to fully investigate metastatic growth within the liver. An alternative approach that significantly minimizes the development of multi-site metastasis is the intrasplenic injection model. Intrasplenic injection delivers tumor cells via the splenic vein that joins with the superior mesenteric vein to become the portal vein<sup>49,50</sup>. Animals can be monitored for outgrowth of metastatic lesions in the liver because formation of metastases at other sites is rare, and as a result, the animal's overall health is maintained<sup>49,50</sup>. However, it is important to note that the intrasplenic model requires splenectomy to avoid splenic tumors<sup>49,50</sup>, a procedure that impacts immune function. For example, myocardial ischemia reperfusion injury is characterized by infiltration of Ly6C<sup>+</sup> monocyte subsets that originate from the spleen and are responsible for phagocytic and proteolytic activity during the wound healing following ischemia<sup>51,52</sup>. With splenectomy, there is an observed reduction in monocyte populations that assist in wound healing<sup>52</sup>. Further, splenectomy has been shown to reduce primary tumor growth and lung metastases in a non-small cell lung cancer model, specifically through a reduction in the number of circulating and intra-tumor CCR2<sup>+</sup>CD11b<sup>+</sup>Ly6C<sup>+</sup> monocytic myeloid cells<sup>53</sup>. Additionally, splenectomy following intrasplenic injection of colon cancer cells resulted in reduced levels of anti-tumor natural killer cells in mesenteric lymph nodes and elevated liver metastasis<sup>54</sup>. In sum, these findings suggest that splenectomy compromises the immune system's role with subsequent consequences for metastatic cell fate.

### Portal Vein Injection Model of Liver Metastasis

To investigate breast cancer metastasis to the liver in a fully immune competent host, under conditions where mice are not compromised due to multi-organ metastases, a portal vein injection model was developed. Intraportal injection models have been used previously to study liver metastasis of colorectal<sup>55,56</sup> and melanoma<sup>16</sup> cell lines; here we describe application of the intraportal injection to model syngeneic mammary tumor cell metastasis. This model can be used to study the later stages of the metastatic cascade including breast cancer cell extravasation and seeding, tumor cell fate decisions regarding death/proliferation/dormancy, and outgrowth into overt lesions. In this model, syngeneic mammary tumor cell lines are injected *via* the portal vein of immune competent Balb/c female mice, a method that delivers tumor cells firstly and directly to the liver without removal of the spleen. To develop this model, the use of four mammary tumor cell lines that range in their metastatic capability from low to high were employed: D2.OR, D2A1, and 4T1, and have employed D2A1 tagged with green fluorescent protein (D2A1-GFP) to investigate early time-points after tumor cell injection. 4T1 is a highly metastatic cell line derived from the 410.4 tumor that spontaneously arose in an MMTV<sup>+</sup> Balb/c female mouse<sup>36,37</sup> and metastasizes to lung, liver, brain, and bone from mammary fat pad primary tumors<sup>39,57,58</sup>. D2A1 tumor cells were also originally derived from a spontaneous mammary tumor arising in a Balb/c host after transplant of D2 hyperplastic alveolar nodule cells, and are confirmed to be metastatic from the primary tumor to the lung<sup>59,60</sup>. D2.OR tumor cells are a non-metastatic sister line to the D2A1 line and, although they escape the primary tumor and arrive at secondary sites, they rarely establish distant metastases<sup>60,61</sup>.

Additionally, it is important to avoid use of commonly employed pain management drugs including non-steroidal anti-inflammatory drugs (NSAIDs) during or following the surgical procedure. NSAIDs have anti-tumor activity in certain breast cancers<sup>62-65</sup>, and some classes of NSAIDs increase the risk of hepatotoxicity<sup>66,67</sup>, potentially compromising the study of liver metastasis and the liver metastatic niche. Further, studies suggest that NSAIDs directly influence the tissue microenvironment, reducing pro-metastatic extracellular matrix proteins tenascin-C<sup>68</sup> and fibrillar collagen<sup>62,65</sup>. Alternatively, the use of an opioid derivative, buprenorphine, was used because of its efficacy in rodent pain management<sup>69</sup> and due to the lack of evidence that opioids have anti-tumor activity<sup>70</sup>. This portal vein injection model was optimized for smaller injection volumes of 5 - 10 µl to avoid unnecessary damage to the liver. The model was also optimized to include needles with smaller diameter (≥ 32 gauge) and use of hemostatic gauze immediately following injection to minimize blood loss during the procedure. In contrast to these optimized injection parameters, cell numbers should be determined on an individual basis, based on the tumorigenic potential of the cell line. However, starting at ≤ 10,000 cells/injection for long-term studies is recommended. For shorter endpoints (e.g., 24 hr post-injection) considerably more tumor cells (e.g., 1 x 10<sup>5</sup> - 1 x 10<sup>6</sup>) may be used if warranted. In summary, the portal vein injection model detailed here represents a useful tool for the study of breast cancer metastasis to the liver and circumvents a number of the limitations of other liver metastasis models. This model facilitates study of tumor cell extravasation, seeding, early fate decisions of survival, proliferation, and dormancy, and metastatic outgrowth in immune competent murine hosts.

## Protocol

All animal procedures in this article were reviewed and approved by the Oregon Health & Science University Institutional Animal Care and Use Committee.

### 1. Preparation of the Surgical Area and Instruments

1. Prepare the scissors, forceps, and hemostat by autoclaving at 124 °C for 30 min, 1 - 2 days prior to the planned surgeries. Ensure access to autoclaved or sterile bedding, cages, and food for post-surgical recovery.
2. Prepare an aseptic surgical area, preferably in a laminar flow hood.

1. Wipe down all surfaces of the surgical area with 10% bleach, including the heating pad, light source, anesthesia tubing and nose cone, and any other part of the surgical suite that will be in close proximity to the surgical procedure while it is being performed.
  2. In the aseptic surgical area, place the cleaned heating pad with sterile drape, light source, anesthesia tubing and nosecone, insulin syringes, 1 ml syringes, bupivacaine, artificial tears, sterile saline, 2 x 2" sterile gauze sponges, 4 x 4" sterile gauze, hemostatic gauze cut into 0.5 - 1 cm<sup>2</sup> pieces, scissors, forceps, hemostat, 4-0 vicryl sutures with taper needle, and 50 ml 2% Chlorhexidine gluconate in an autoclaved container.
  3. Ensure that there is room in this space for prepared tumor cells stored on ice.
  4. On the bench adjacent to the surgical area, prepare the recovery area with a second heating pad and clean cages with sterile bedding.
- NOTE: This area can also house items such as a bead sterilizer.

## 2. Portal Vein Injection

1. One-hour prior to the planned injections, treat Balb/c female mice aged 8 - 15 weeks with 100 µl of 0.015 mg/ml buprenorphine, subcutaneously, for pain management.  
NOTE: This injection protocol may be applied to any strain of female or male mouse at any age, using the appropriate cell lines for changes to the strain.
2. Prepare the tumor cells for injection based on protocols for the cell line or tumor explant of choice. Test all tumor cell lines prior to administration for the presence of murine pathogens to reduce the risk of introducing such pathogens into the animal colony.
  1. For syngeneic Balb/c tumor cell lines including D2A1, D2.OR, and 4T1 tumor cells, thaw cells into a 10 cm tissue culture plate 3 days prior to injection such that the following day cells are at ~ 90 - 100% confluency.
  2. 1 day following tumor cell thaw wash cells once with 1x phosphate buffered saline (PBS) and trypsinize the confluent tumor cells using 2 ml of 0.05% trypsin at 37 °C for 5 min. Add 8 ml of complete media (DMEM high glucose, 10% fetal bovine serum, 2 mM L-glutamine, and 1x penicillin/streptomycin) and passage 1:10 into a fresh 10 cm dish with 10 ml of complete media.
  3. On the day of the injections, wash cells once with 1x PBS and trypsinize as described above.
  4. Resuspend trypsinized cells in 8 ml of complete media, spin for 5 min at 1,500 x g, remove the media and resuspend in 5 ml 1x PBS.
  5. Count cells on a hemocytometer using trypan blue exclusion for viability assessment. Resuspend cells for injection in 1x PBS at a pre-determined concentration and volume.  
NOTE: 5 - 10 µl is recommended as smaller injection volumes prevent unnecessary damage to the liver.
  6. Keep cells on ice for the duration of the injections. Following completion of injections, return a sample of cells to the laboratory and place in culture in complete media for 1 day to ensure viability.
3. Place the mouse under anesthesia with 2 - 2.5% isoflurane (2-chloro-2-(difluoromethoxy)-1,1,1-trifluoro-ethane) delivered in oxygen. Maintain body temperature using the heating pad. Ensure complete anesthetization by assessing for a reaction to a toe pinch, and then maintain anesthesia at 2 - 2.5% isoflurane.  
NOTE: It is important to monitor the animals breathing rate and adjust the isoflurane flow-rate accordingly throughout the procedure.
4. Place a small amount of artificial tears or vet ointment over each eye to avoid excessive drying of the eyes during the surgical procedure.
5. Place the mouse in a supine position, on its back with abdomen exposed.
6. Remove hair on the ventral left side of the rodent from the second rib space down to the 4<sup>th</sup> inguinal mammary gland nipple by wiping the area with chemical depilatory. Allow the depilatory to sit for 1 - 2 min and then remove completely with gauze and H<sub>2</sub>O. This step can be done 1 - 2 days in advance to save time if numerous surgeries are planned.
7. Take one 2 x 2" sterile gauze sponge (soaked in 2% Chlorhexidine) and wipe down the mouse at the site of hair removal. Sterilize the entire surrounding area, including the tail, to minimize bacterial contamination of instruments.
8. Wipe the site of hair removal and surrounding area down with an alcohol prep pad.
9. Repeat 2% Chlorhexidine and alcohol steps once more and finish with a final Chlorhexidine wipe down for a total of three 2% Chlorhexidine and two alcohol prep pad washes. Do the final Chlorhexidine wipe such that the chemical is not dripping around the surgical site to avoid getting Chlorhexidine on internal organs. NOTE: Application of large amounts of chlorhexidine and alcohol to the skin and surrounding fur may result in a significant drop in body temperature. Do not wipe with excess volume during steps 2.7-2.9. Maintain body temperature with a heating pad.
10. Using sterile gloves and a sterilized scalpel with sterile blade, make a single 1-inch incision into the skin between the median and sagittal planes on the left side of the mouse, starting just below the ribs and ending just above the plane of the fourth inguinal mammary gland teat.
11. Using autoclaved or bead sterilized scissors and forceps, make a similar 1-inch incision into the peritoneum. Avoid cutting into the mammary fat pad and ensure not to cut the intestines, liver, or diaphragm.
12. Place a 4 x 4" gauze pad soaked in sterile saline on the left side of the mouse, where the incision was made, such that internal organs can be placed on the gauze and not come into contact with the surrounding skin or surgical area.
13. Prepare tumor cells by pipetting up and down several times as tumor cells will settle during preparation of the mouse. Prepare a 25 µl removable needle syringe and 32-gauge needle with tumor cells. Push on the syringe until tumor cells are at the tip of the needle and the plunger is at the appropriate volume for injection; avoid injection of air bubbles.
14. Wipe the outside of the needle with a sterile alcohol pad to remove any external tumor cells. Use caution to avoid needle sticks.
15. Hold the median side of the incision, including skin and peritoneal lining, aside with the forceps and use a sterile cotton swab to carefully pull the large and small intestines out, placing them on the sterile gauze soaked in sterile saline. Pull out large and small intestines until the portal vein is visualized.
16. Cover the internal organs in the saline soaked gauze to maintain internal moisture and sterility.
17. Have an assistant, also wearing sterile gloves, hold the intestines wrapped in the saline soaked gauze gently out of the way with a sterile cotton tipped swab to fully reveal the portal vein. Additionally, it may be necessary to use the autoclaved hemostat or forceps to hold tissue aside on the median side of the incision.
18. Insert the needle loaded with tumor cells ~ 3 - 5 mm into the portal vein ~ 10 mm below the liver at an angle < 5° to the vein, with bevel facing up. Slowly inject the full volume containing tumor cells. Allow blood to flow past the needle head for several seconds to avoid back flow of tumor cells out of the vein. Minimize moving the needle in the vein during the injection. Again, use caution to avoid needle sticks.

NOTE: Visualization of the portal vein is done without magnification, however a stereo microscope may be used if preferred.

19. Remove the needle while simultaneously placing a sterile cotton tip applicator on the vein with pressure. With the assistant still holding the intestines aside place one piece of 0.5 - 1 cm<sup>2</sup> hemostatic gauze over the injection site on the vein.  
NOTE: Hemostatic powder was also attempted for this step in the protocol but was not effective in stopping venous blood loss following injection.
20. Hold the hemostatic gauze at the injection site with pressure from a sterile cotton tip applicator for 5 min.
21. Assess closure of the vein by carefully lifting the hemostatic gauze, if the gauze sticks to the surrounding tissue, a small amount of sterile saline can be used to soak and lift the gauze.
22. If blood loss occurs at this time, place an additional piece of hemostatic gauze at the site with pressure for an additional 5 min. When blood flow has ceased completely, remove the gauze from the mouse.  
NOTE: Blood loss during the surgical procedure must be carefully assessed and if the total allowed blood loss volume is met or exceeded (based on regulatory standard operating procedures for the investigator's institutional review boards) the mouse must be euthanized while under anesthesia by cardiac perfusion.
23. Once the injection site is deemed intact, with no blood leaving the injection site, place the internal organs gently back into the abdominal cavity.
24. Suture the peritoneal lining and then the skin with sterile 4-0 vicryl suture and taper needle using a simple continuous or interrupted suture pattern. Typically, closing the incision requires 10-15 sutures.
25. Inject 100 µl of bupivacaine (5 mg/ml) along the incision site for local pain management using an insulin syringe. Inject 0.5 ml of sterile saline subcutaneously using a 1 ml syringe with 26-gauge needle for hydration. Surgeries take 15 - 25 min to complete.
26. To maintain sterile conditions throughout the surgery, ensure that all tools and materials coming into contact with the mouse, including gloved hands, are cleaned appropriately prior to contact. Where possible use sterile materials and gloves, or minimally utilize a 70% ethanol solution or 10% bleach solution to clean.
27. If multiple surgeries are planned for a single session remake the initial surgical area with fresh sterile drape, insulin syringes, 1 ml syringes, sterile saline, 2 x 2" sterile gauze sponges, 4 x 4" sterile gauze, hemostatic gauze cut into 0.5 - 1 cm<sup>2</sup> pieces, 4-0 vicryl sutures with taper needle, and 2% Chlorhexidine. Bead-sterilize the scissors, forceps, and hemostat in between surgeries and allow to adequately cool prior to re-use.

### 3. Recovery, Monitoring Rodent Health, and End-point Analyses

1. After the surgical procedure is complete, maintain mice on a heating pad for recovery in bedding-free, clean cages for a minimum of 20 min. Mice typically take 2 - 4 min to wake up from anesthesia.
2. Do not return an animal that has undergone surgery to co-habitation with other animals until it has fully recovered from anesthesia. Do not leave an animal unattended while it is regaining consciousness and monitor until the animal has regained the ability to maintain itself in sternal recumbency.
3. Give mice 0.05 - 0.1 mg/kg buprenorphine for pain management every 6-12 hr following surgery, for up to 72 hr.
4. Check sutures daily to ensure they remain intact during healing. In the case that sutures come undone, place the mouse under anesthesia, remove remaining sutures, and replace. In the case of infection or inflammation consult veterinarian staff.  
NOTE: Infection or inflammation has not been encountered with this protocol.
5. For metastasis studies, perform daily health checks until outward signs of metastatic disease are observed including, but not limited to: >10% weight loss/gain, scruffiness, loss of attention to surroundings, abdominal edema/ascites, pale eyes and ears, or a hunched position.  
NOTE: Daily health checks are particularly important when developing the model for use with a new cell line or cell concentration until the timeline of metastasis is well understood.
6. At study end-point, euthanize mice by CO<sub>2</sub> inhalation followed by cervical dislocation.  
NOTE: Alternative methods of euthanasia approved by the investigators' oversight committee may be used, including perfusion with 1x PBS while under anesthesia. Perfusion of the liver is performed by cannulating the portal vein, snipping the inferior vena cava, and pushing 1x PBS through the liver vasculature at a rate of 4 ml/min for 1 - 2 min to remove circulating blood and leukocytes.  
NOTE: Depending on the endpoint for the study, the cell line, and the concentration used, overt liver metastasis may or may not be apparent at necropsy. Micrometastatic lesions may be revealed with histological analysis of the liver. Endpoints will vary based on the study design.
7. Extract the liver with scissors and forceps by first removing the gallbladder, then cut through the inferior vena cava superior to the liver. Cut through the vena cava, portal vein, and hepatic artery inferior to the liver.
8. Remove the whole liver gently and wash 5x in 1x PBS.
9. Separate the liver into left, right, median, and caudate lobes.
10. Formalin fix liver in 10% neutral buffered formalin for 48 hr while shaking at room temperature. Process tissues through a series of alcohols in increasing concentration and xylene; paraffin embed the fixed tissue<sup>71</sup>.  
NOTE: Alternatively, the liver may be snap-frozen by placing tissue in a cryomold with optimum cutting temperature (OCT) formula and freezing on dry ice pellets submerged in 95% ethanol.
  1. Using a microtome, cut into the paraffin embedded tissue block such that a match-head size of tissue is revealed.
  2. Cut five 4-micron serial sections, this constitutes the first level for analysis.
  3. Cut through 250 microns of tissue, throw these sections in the waste.
  4. At 250 microns cut a second level of five 4-micron serial sections.
  5. Repeat as necessary to section through the entire liver. Hematoxylin and eosin stain the first section of every level to assess for metastasis<sup>72</sup>.  
NOTE: For snap-frozen tissue use a cryostat to cut sections.  
NOTE: Detection of micrometastatic disease will require tumor cell specific staining.
11. Remove mice from study if there is tumor growth at the incision site, as this indicates tumor cell leakage into the peritoneal cavity following injection.  
NOTE: This problem has not been observed.

## Representative Results

The portal vein injection model, in which tumor cells are delivered directly to the liver via a surgical procedure, allows for tumor cell injection into the portal vein. Under antiseptic conditions, in an anesthetized mouse, a ~1-inch surgical incision is made on the left side of the mouse between the median and sagittal planes, starting just above the plane of the fourth inguinal mammary gland teat and ending just below the ribs. The large and small intestines are gently pulled through the incision to provide visualization of the portal vein (**Figure 1A**). Accurate anatomical identification of the portal vein and successful intra-portal injection can be confirmed by practicing the injection protocol with India ink or a similar dye. Correct injection via the portal vein will result in the ink being delivered immediately and specifically to the liver, and will not result in India ink spread to the lung (**Figure 1B**). Further, using D2A1 mouse mammary tumor cells tagged with GFP, dispersal of tumor cells throughout the liver is apparent at ninety minutes post-injection, confirming portal vein injection delivery to the liver (**Figure 1C**). At higher magnification it becomes apparent that at 90 min post-injection, tumor cells are found within sinusoids, as well as within the liver parenchyma in close proximity to portal triads, where the portal vein blood enters the liver (**Figure 1C**). These data suggest that active tumor cell extravasation is occurring at 90 min post-tumor cell injection. Taken together, these data confirm that the portal vein injection model delivers the injection volume directly to the liver, with ink or tumor cells dispersed throughout the liver and no appreciable transport of injection volume to the lung.

To assess robustness of the portal vein injection model, three separate syngeneic mouse mammary tumor cell lines were tested in adult female Balb/c mice. These mammary tumor lines were selected based on their characterized behavior in mammary fat pad models and include the highly aggressive and metastatic 4T1 cell line, the less aggressive metastatic D2A1 line, and the low/non-metastatic D2.OR line<sup>37,61,73,74</sup>. 2,000 and 10,000 cells per injection were tested with no notable differences in the time to development of overt metastasis with these low cell concentrations. For these studies surrogate markers of metastasis were used such as lack of grooming, pallor, and weight loss to justify necropsy, upon which the presence or absence of liver metastases were confirmed by visual assessment of the liver and other organs to confirm intra-portal delivery. These data confirm previous reports that the 4T1 and D2A1 cell lines represent more aggressive mammary tumor lines, as shorter metastasis free survival rates are observed compared to mice injected with the less aggressive D2.OR line (**Figure 2A**). Mice injected with 4T1 or D2A1 tumor cells developed overt liver metastasis by ~ 30 - 40 days post-injection, and some developed metastasis as early as 18 days post-injection (**Figure 2A**), whereas only one mouse injected with D2.OR cells had developed overt liver metastasis by study end, which was 60 - 65 days post-tumor cell injection. Metastases were subsequently confirmed by sectioning through the liver in 250  $\mu$ m levels and analyzing hematoxylin and eosin (H&E) stained sections (**Figure 2B-D**).

In addition to detection of overt metastatic lesions in the mouse liver, the portal vein model can also be utilized to study earlier events in the metastatic cascade including detection of single cells/cell clusters following extravasation, and formation of micro-metastatic lesions. Multiplex immunofluorescence-staining was used to detect 4T1, D2A1, and D2.OR mammary tumor cells in liver when they are present as single cells or micro-metastatic lesions, as H&E is not sufficient to confirm the presence of small lesions. **Figure 3A** shows a representative Balb/c mouse liver with a putative micrometastatic foci of D2A1 tumor cells that are positive for the epithelial keratin CK18, negative for the pan-immune marker CD45, and negative for the hepatocyte marker Heppar-1. Hepatocytes also stain positive for CK18, necessitating use of Heppar-1 in this staining panel. One important note is that bile duct epithelium and liver progenitor cells stain positive for CK18, requiring careful discrimination between tumor cells and bile ducts, particularly when assessing periportal regions (**Figure 3A**). An alternative to multiplex immunofluorescence to identify single disseminated cells and micrometastatic foci is to utilize syngeneic mammary tumor lines tagged with enhanced green fluorescent protein (eGFP) and/or luciferase and perform IHC for the tag (**Figure 1C**). Due to the immunogenicity of eGFP, luciferase, and other proteins, it is essential to use mouse models that are tolerized to these proteins, such as the novel immune competent "glowing head" mouse that expresses eGFP and luciferase in the anterior pituitary gland<sup>75</sup>. For identification of macrometastatic lesions of untagged syngeneic lines such as the D2A1 tumor line, the CK18/Heppar-1/CD45 multiplex immunofluorescence is ideal (**Figure 3B**).



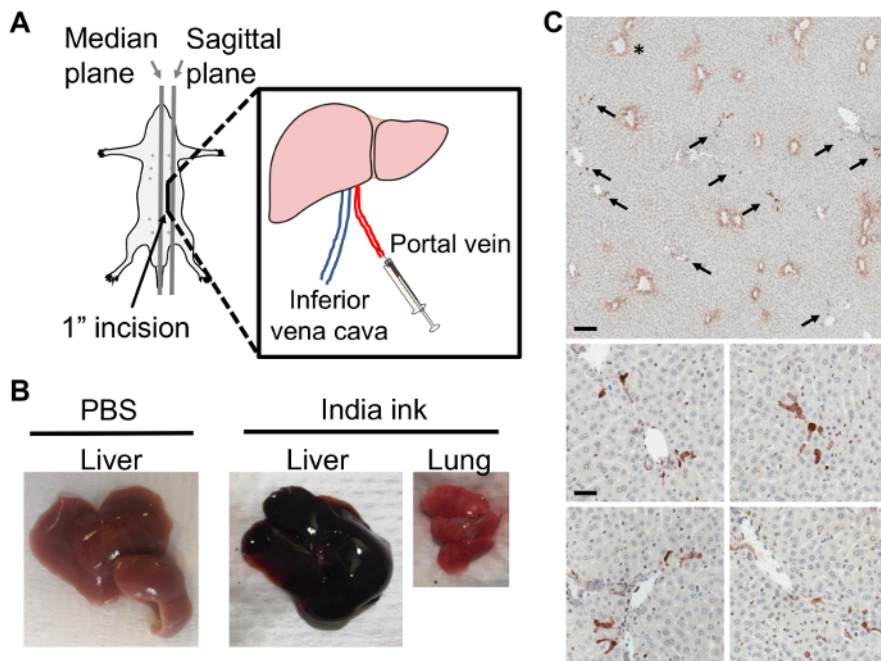


**Figure 1: Portal Vein Injection Delivers Tumor Cells Directly to the Liver.** **A)** Portal vein injection; the incision is made between the median and left sagittal planes, from above the plane of the fourth inguinal mammary gland teat and ending just below the rib cage. **B)** Balb/c liver with PBS injection (left). Following India ink injection via the portal vein, the liver (middle) but not the lung (right) takes up ink. **C)** Representative thin section images of D2A1 mouse mammary tumor cells tagged with GFP in a Balb/c mouse liver at 90 min post-injection of  $1 \times 10^6$  tumor cells via the portal vein. Livers were formalin fixed, paraffin embedded, sectioned, and stained with anti-GFP antibody for tumor cell detection. Top panel shows dark brown stained tumor cells (arrows) dispersed throughout the liver, asterisk denotes non-specific hepatocyte staining around central veins; scale bar = 300  $\mu\text{m}$ . Lower panels show representative images of tumor cells at 90 min post-injection still closely associated with vasculature; scale bar = 50  $\mu\text{m}$ . [Please click here to view a larger version of this figure.](#)

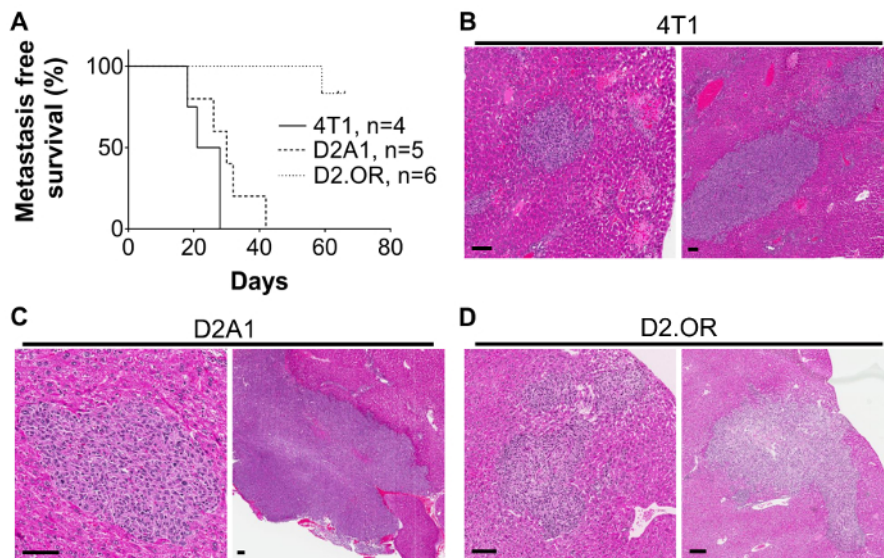


**Figure 2: Outgrowth of Mouse Mammary Tumor Cell Lines in the Liver Following Portal Vein Injection.** **A)** Kaplan-Meier curve showing metastasis-free survival rates in mice injected with 2,000-10,000 4T1, D2A1, or D2.OR mouse mammary tumor cells. Mice were injected with tumor cells and monitored for signs of metastasis including lack of grooming, pale eyes, and weight changes. Metastasis was confirmed at time of necropsy and by H&E on histological sections of the livers. N= 2 4T1 2,000 cells; 2 4T1 10,000 cells. N= 2 D2A1 2,000 cells; 3 D2A1 10,000 cells. N= 3 D2.OR 2,000 cells; 3 D2.OR 10,000 cells. Representative H&E images of **B)** 4T1 lesions at 21 days post-injection of 10,000 cells, **C)** D2A1 lesions at 26 days post-injection of 10,000 tumor cells, and **D)** D2.OR lesions at 59 days post-injection of 10,000 cells; scale bars = 75  $\mu\text{m}$ . Similar lesions are observed when 2,000 4T1 or D2A1 tumor cells were injected. No lesions were detected with 2,000 D2.OR cells. No evidence of metastasis in other organs or at the surgical incision site was apparent in any mouse on these studies. [Please click here to view a larger version of this figure.](#)

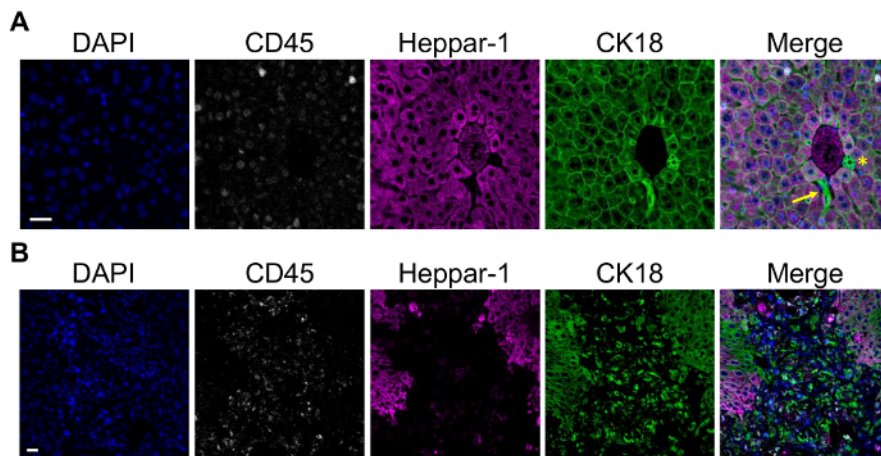


**Figure 3: Detection of Single Cells and Metastatic Lesions in the Mouse Liver using Multiplex Immunofluorescence. A)** Representative multiplex immunofluorescence of D2A1 tumor cells in a Balb/c mouse liver at 90 min post-injection using the portal vein injection model. Staining was done using a multiplex kit. From left to right shows DAPI; CD45 to mark leukocytes; Heppar-1 to mark hepatocytes; and CK18 to mark tumor cells, hepatocytes, and bile duct epithelium. Merged image shows a putative cluster of CK18<sup>+</sup>Heppar-1<sup>-</sup>CD45<sup>-</sup> D2A1 tumor cells closely associated with a portal triad. Arrow = D2A1 tumor cells, asterisk = bile duct epithelium; scale bar = 25  $\mu$ m. **B)** A representative overt D2A1 metastatic lesion using the same staining panel as in A. Tumor cells are CK18<sup>+</sup> whereas adjacent hepatocytes are CK18<sup>+</sup>Heppar-1<sup>+</sup>; scale bar =25  $\mu$ m. Images were captured on a microscope with 20 x 0.8, 40 x 1.3, and 60 x 1.4 objectives and CCD camera, using the microscope software. [Please click here to view a larger version of this figure.](#)

## Discussion

The Balb/c mouse portal vein injection model permits the study of mammary cancer lesions in the liver in the absence of confounding multi-organ metastasis and in a fully immune competent host. Our protocol is an advancement of previously published surgical procedures that permit access to the portal vein for injection of tumor cells directly into the liver<sup>16,55,56</sup>. One advancement we have made is to significantly reduce the number of injected tumor cells from  $\geq 1 \times 10^5$  cells/injection<sup>16,55,56</sup> down to  $\leq 10,000$  tumor cells/injection. We have also expanded the model for the study of breast cancer metastasis to the liver. Using this protocol, two mammary cancer cell lines with known metastatic potential develop liver metastases with shorter latency than a more quiescent mammary tumor cell line. Further, at early time points, tumor cells are distributed throughout the liver parenchyma as single or small groups of single cells after tumor cell injection. The model is poised to address questions of metastatic efficiency including tumor cell extravasation, cell survival, dormancy, and proliferation — all phenotypes that contribute to the development of micro-metastatic and overt metastatic disease in the liver.

It is important to consider numerous aspects of the portal vein injection protocol prior to initiating studies. Carefully deciding on cell lines, cell concentration, total cell number, and end-points of interest based on smaller exploratory studies is highly recommended. Further, the use of immune competent hosts and syngeneic cell lines is of utmost importance for understanding host-tumor cell interactions. The newly developed "glowing head" mouse that expresses eGFP and luciferase from the anterior pituitary gland is an important tool for eliminating host responses to exogenous eGFP and luciferase, proteins often used to tag mammary tumor lines<sup>75</sup>. Use of the "glowing head" mouse and syngeneic tagged tumor cells will facilitate easy identification of single disseminated cells and micrometastatic foci by IHC without the concern of inflammatory responses to eGFP or luciferase. Similarly, choosing pain management strategies carefully to ensure minimal anti- or pro-tumor impact from the drug treatment regimen is strongly recommended. Critical steps in this protocol include maintaining sterile conditions throughout surgeries to ensure that infection does not occur, as this will confound any results. It is also important that the needle is properly placed in the portal vein to ensure that tumor cells are delivered to the liver. Practicing the protocol with dyes such as India ink will help with this issue. Tumor growth at the skin incision site is the best indicator that improper needle placement occurred. Finally, it is critical that blood loss from the portal vein is adequately controlled and ceases entirely prior to suturing the animal. The use of hemostatic gauze greatly diminishes the risk of uncontrolled blood loss from the portal vein following injection. In our hands, procedural related mortality due to blood loss from the portal vein following injection was reduced from 30% to 2% of mice with the use of hemostatic gauze.

It is important to note that the portal vein injection model does not replicate the full metastatic cascade, but is limited to the study of tumor cell extravasation, tumor cell-niche interactions following extravasation and tumor growth. Models that accurately replicate the full metastatic cascade to the liver, such as occurs in patients, are urgently needed. An additional limitation of the portal vein injection model is that it is confounded by the impact of surgery on the host, with wound healing known to impact disease progression<sup>76,77</sup>.

The portal vein injection model represents an improvement on other injection models to study liver metastasis, including intracardiac and intrasplenic models. Specifically, the portal vein injection model allows for the study of a larger range of disease progression than the intracardiac model, which is often limited by concomitant metastases in other tissues. Further, the portal vein model is not complicated by removal of the spleen, as is done in the intrasplenic model.

The portal vein injection model may prove a useful tool for the study of liver metastasis in general. Liver metastasis is the most frequent site of metastasis in adenocarcinomas overall, with particularly high rates in pancreatic cancers (85% of metastases are to the liver), colon and rectal adenocarcinomas (>70%), as well as stomach and esophageal (>30%)<sup>1</sup>. Although spontaneous and orthotopic primary tumor models of pancreatic and colon adenocarcinomas more readily metastasize to the liver<sup>78,79</sup>, the portal vein injection model may prove useful to understanding the metastatic process of these cancers as controlled delivery of tumor cells permits biochemical, molecular and histological

assessments at specified times after tumor cell arrival. In summary, the portal vein injection model represents an important improvement on available liver metastasis models of breast cancer, and may also be applicable to the liver metastasis field in general.

## Disclosures

The authors have nothing to disclose and declare no competing financial interests.

## Acknowledgements

The authors would like to acknowledge Alexandra Quackenbush for assisting with surgical procedures during filming of the video protocol, Hadley Holden for histological support, Sonali Jindal for input on tumor and liver pathology during method development, and Breanna Caruso for critical review of the manuscript. The D2A1 and D2.OR mammary tumor cells were a gift from Dr. Ann Chambers, the D2A1-GFP tumor cells were a gift from Dr. Jeffrey Green, and the 4T1 tumor cells were a gift from Dr. Heide Ford. The OHSU Advanced Light Microscopy Core at the Jungers Center was utilized for imaging. The work included in this manuscript includes funding from NIH/NCI NRSA F31CA186524 (to ETG) and NIH/NCI 5R01CA169175 (to PS).

## References

- Hess, K. R. *et al.* Metastatic patterns in adenocarcinoma. *Cancer*. **106**, 1624-1633 (2006).
- Berman, A. T., Thukral, A. D., Hwang, W. T., Solin, L. J., & Vapiwala, N. Incidence and patterns of distant metastases for patients with early-stage breast cancer after breast conservation treatment. *Clin Breast Cancer*. **13**, 88-94 (2013).
- Savci-Heijink, C. D. *et al.* Retrospective analysis of metastatic behaviour of breast cancer subtypes. *Breast Cancer Res Treat*. **150**, 547-557 (2015).
- Gerratana, L. *et al.* Pattern of metastasis and outcome in patients with breast cancer. *Clin Exp Metastasis*. **32**, 125-133 (2015).
- Bonotto, M. *et al.* Measures of outcome in metastatic breast cancer: insights from a real-world scenario. *Oncologist*. **19**, 608-615 (2014).
- Wyld, L. *et al.* Prognostic factors for patients with hepatic metastases from breast cancer. *Br J Cancer*. **89**, 284-290 (2003).
- Tarhan, M. O. *et al.* The clinicopathological evaluation of the breast cancer patients with brain metastases: predictors of survival. *Clin Exp Metastasis*. **30**, 201-213 (2013).
- Tseng, L. M. *et al.* Distant metastasis in triple-negative breast cancer. *Neoplasma*. **60**, 290-294 (2013).
- Liu, X. H., Man, Y. N., Cao, R., Liu, C., & Wu, X. Z. Individualized chemotherapy based on organ selectivity: a retrospective study of vinorelbine and capecitabine for patients with metastatic breast cancer. *Curr Med Res Opin*. **30**, 1017-1024 (2014).
- Ahn, S. G. *et al.* Prognostic factors for patients with bone-only metastasis in breast cancer. *Yonsei medical journal*. **54**, 1168-1177 (2013).
- Purushotham, A. *et al.* Age at diagnosis and distant metastasis in breast cancer—a surprising inverse relationship. *Eur J Cancer*. **50**, 1697-1705 (2014).
- Karimi, A., Delpisheh, A., Sayehmiri, K., Saboori, H., & Rahimi, E. Predictive factors of survival time of breast cancer in kurdistan province of Iran between 2006-2014: a cox regression approach. *Asian Pac J Cancer Prev*. **15**, 8483-8488 (2014).
- Chambers, A. F., Groom, A. C., & MacDonald, I. C. Dissemination and growth of cancer cells in metastatic sites. *Nat Rev Cancer*. **2**, 563-572 (2002).
- Pantel, K., & Brakenhoff, R. H. Dissecting the metastatic cascade. *Nature reviews. Cancer*. **4**, 448-456 (2004).
- Joyce, J. A., & Pollard, J. W. Microenvironmental regulation of metastasis. *Nat Rev Cancer*. **9**, 239-252 (2009).
- Luzzi, K. J. *et al.* Multistep nature of metastatic inefficiency: dormancy of solitary cells after successful extravasation and limited survival of early micrometastases. *Am J Pathol*. **153**, 865-873 (1998).
- Cameron, M. D. *et al.* Temporal progression of metastasis in lung: cell survival, dormancy, and location dependence of metastatic inefficiency. *Cancer Res*. **60**, 2541-2546 (2000).
- Psaila, B., & Lyden, D. The metastatic niche: adapting the foreign soil. *Nat Rev Cancer*. **9**, 285-293 (2009).
- Oskarsson, T. *et al.* Breast cancer cells produce tenascin C as a metastatic niche component to colonize the lungs. *Nat Med*. **17**, 867-874 (2011).
- Costa-Silva, B. *et al.* Pancreatic cancer exosomes initiate pre-metastatic niche formation in the liver. *Nat Cell Biol*. **17**, 816-826 (2015).
- Kaplan, R. N. *et al.* VEGFR1-positive haematopoietic bone marrow progenitors initiate the pre-metastatic niche. *Nature*. **438**, 820-827 (2005).
- Erler, J. T. *et al.* Hypoxia-induced lysyl oxidase is a critical mediator of bone marrow cell recruitment to form the premetastatic niche. *Cancer Cell*. **15**, 35-44 (2009).
- Zhao, L. *et al.* Recruitment of a myeloid cell subset (CD11b/Gr1 mid) via CCL2/CCR2 promotes the development of colorectal cancer liver metastasis. *Hepatology*. **57**, 829-839 (2013).
- Peinado, H., Lavotshkin, S., & Lyden, D. The secreted factors responsible for pre-metastatic niche formation: old sayings and new thoughts. *Semin Cancer Biol*. **21**, 139-146 (2011).
- Van den Eynden, G. G. *et al.* The multifaceted role of the microenvironment in liver metastasis: biology and clinical implications. *Cancer Res*. **73**, 2031-2043 (2013).
- Kang, Y. *et al.* A multigenic program mediating breast cancer metastasis to bone. *Cancer Cell*. **3**, 537-549 (2003).
- Minn, A. J. *et al.* Genes that mediate breast cancer metastasis to lung. *Nature*. **436**, 518-524 (2005).
- Bos, P. D. *et al.* Genes that mediate breast cancer metastasis to the brain. *Nature*. **459**, 1005-1009 (2009).
- Ogba, N. *et al.* Luminal breast cancer metastases and tumor arousal from dormancy are promoted by direct actions of estradiol and progesterone on the malignant cells. *Breast cancer research : BCR*. **16**, 489 (2014).
- Coffelt, S. B. *et al.* IL-17-producing gammadelta T cells and neutrophils conspire to promote breast cancer metastasis. *Nature*. **522**, 345-348 (2015).
- Kitamura, T., Qian, B. Z., & Pollard, J. W. Immune cell promotion of metastasis. *Nat Rev Immunol*. **15**, 73-86 (2015).
- Zhang, Q. *et al.* CCL5-Mediated Th2 Immune Polarization Promotes Metastasis in Luminal Breast Cancer. *Cancer Res*. **75**, 4312-4321 (2015).



33. Ruffell, B., & Coussens, L. M. Macrophages and therapeutic resistance in cancer. *Cancer Cell*. **27**, 462-472 (2015).
34. Koyama, S. *et al.* Adaptive resistance to therapeutic PD-1 blockade is associated with upregulation of alternative immune checkpoints. *Nat Commun*. **7**, 10501 (2016).
35. Quail, D. F. *et al.* The tumor microenvironment underlies acquired resistance to CSF-1R inhibition in gliomas. *Science*. **352**, aad3018 (2016).
36. Dexter, D. L. *et al.* Heterogeneity of tumor cells from a single mouse mammary tumor. *Cancer Res*. **38**, 3174-3181 (1978).
37. Aslakson, C. J., & Miller, F. R. Selective events in the metastatic process defined by analysis of the sequential dissemination of subpopulations of a mouse mammary tumor. *Cancer Res*. **52**, 1399-1405 (1992).
38. Fantozzi, A., & Christofori, G. Mouse models of breast cancer metastasis. *Breast Cancer Res*. **8**, 212 (2006).
39. Pulaski, B. A., & Ostrand-Rosenberg, S. Reduction of established spontaneous mammary carcinoma metastases following immunotherapy with major histocompatibility complex class II and B7.1 cell-based tumor vaccines. *Cancer Res*. **58**, 1486-1493 (1998).
40. Doornebal, C. W. *et al.* A preclinical mouse model of invasive lobular breast cancer metastasis. *Cancer Res*. **73**, 353-363 (2013).
41. Derksen, P. W. *et al.* Somatic inactivation of E-cadherin and p53 in mice leads to metastatic lobular mammary carcinoma through induction of anoikis resistance and angiogenesis. *Cancer Cell*. **10**, 437-449 (2006).
42. Pravtcheva, D. D., & Wise, T. L. Metastasizing mammary carcinomas in H19 enhancers-Igf2 transgenic mice. *J Exp Zool*. **281**, 43-57 (1998).
43. Lin, S. C. *et al.* Somatic mutation of p53 leads to estrogen receptor alpha-positive and -negative mouse mammary tumors with high frequency of metastasis. *Cancer Res*. **64**, 3525-3532 (2004).
44. Basse, P., Hokland, P., Heron, I., & Hokland, M. Fate of tumor cells injected into left ventricle of heart in BALB/c mice: role of natural killer cells. *J Natl Cancer Inst*. **80**, 657-665 (1988).
45. Campbell, J. P., Merkel, A. R., Masood-Campbell, S. K., Eleftheriou, F., & Sterling, J. A. Models of bone metastasis. *J Vis Exp.*, e4260 (2012).
46. Balathasan, L., Beech, J. S., & Muschel, R. J. Ultrasonography-guided intracardiac injection: an improvement for quantitative brain colonization assays. *The American journal of pathology*. **183**, 26-34 (2013).
47. Werbeck, J. L. *et al.* Tumor microenvironment regulates metastasis and metastasis genes of mouse MMTV-PyMT mammary cancer cells in vivo. *Vet Pathol*. **51**, 868-881 (2014).
48. Zhou, H., & Zhao, D. Ultrasound imaging-guided intracardiac injection to develop a mouse model of breast cancer brain metastases followed by longitudinal MRI. *J Vis Exp*. (2014).
49. Rajendran, S. *et al.* Murine bioluminescent hepatic tumour model. *J Vis Exp*. (2010).
50. Soares, K. C. *et al.* A preclinical murine model of hepatic metastases. *J Vis Exp.*, 51677 (2014).
51. Nahrendorf, M. *et al.* The healing myocardium sequentially mobilizes two monocyte subsets with divergent and complementary functions. *J Exp Med*. **204**, 3037-3047 (2007).
52. Swirski, F. K. *et al.* Identification of splenic reservoir monocytes and their deployment to inflammatory sites. *Science*. **325**, 612-616 (2009).
53. Levy, L. *et al.* Splenectomy inhibits non-small cell lung cancer growth by modulating anti-tumor adaptive and innate immune response. *Oncoimmunology*. **4**, e998469 (2015).
54. Higashijima, J. *et al.* Effect of splenectomy on antitumor immune system in mice. *Anticancer Res*. **29**, 385-393 (2009).
55. Thalheimer, A. *et al.* The intraportal injection model: a practical animal model for hepatic metastases and tumor cell dissemination in human colon cancer. *BMC Cancer*. **9**, 29 (2009).
56. Limani, P. *et al.* Selective portal vein injection for the design of syngeneic models of liver malignancy. *Am J Physiol Gastrointest Liver Physiol*. **310**, G682-688 (2016).
57. Lelekakis, M. *et al.* A novel orthotopic model of breast cancer metastasis to bone. *Clin Exp Metastasis*. **17**, 163-170 (1999).
58. Pulaski, B. A., & Ostrand-Rosenberg, S. Mouse 4T1 breast tumor model. *Current protocols in immunology / edited by John E. Coligan ... [et al.]*. Unit 20 22 (2001).
59. Mahoney, K. H., Miller, B. E., & Heppner, G. H. FACS quantitation of leucine aminopeptidase and acid phosphatase on tumor-associated macrophages from metastatic and nonmetastatic mouse mammary tumors. *J Leukoc Biol*. **38**, 573-585 (1985).
60. Rak, J. W., McEachern, D., & Miller, F. R. Sequential alteration of peanut agglutinin binding-glycoprotein expression during progression of murine mammary neoplasia. *Br J Cancer*. **65**, 641-648 (1992).
61. Barkan, D. *et al.* Metastatic growth from dormant cells induced by a col-I-enriched fibrotic environment. *Cancer Res*. **70**, 5706-5716 (2010).
62. Lyons, T. R. *et al.* Postpartum mammary gland involution drives progression of ductal carcinoma in situ through collagen and COX-2. *Nat Med*. **17**, 1109-1115 (2011).
63. Allott, E. H. *et al.* Non-steroidal anti-inflammatory drug use, hormone receptor status, and breast cancer-specific mortality in the Carolina Breast Cancer Study. *Breast Cancer Res Treat*. **147**, 415-421 (2014).
64. Kim, S. *et al.* Lifetime use of nonsteroidal anti-inflammatory drugs and breast cancer risk: results from a prospective study of women with a sister with breast cancer. *BMC Cancer*. **15**, 960 (2015).
65. Esbona, K. *et al.* COX-2 modulates mammary tumor progression in response to collagen density. *Breast Cancer Res*. **18**, 35 (2016).
66. Andrade, R. J. *et al.* Drug-induced liver injury: an analysis of 461 incidences submitted to the Spanish registry over a 10-year period. *Gastroenterology*. **129**, 512-521 (2005).
67. Chalasani, N. *et al.* Causes, clinical features, and outcomes from a prospective study of drug-induced liver injury in the United States. *Gastroenterology*. **135**, 1924-1934, 1934 e1921-1924 (2008).
68. O'Brien, J. *et al.* Non-steroidal anti-inflammatory drugs target the pro-tumorigenic extracellular matrix of the postpartum mammary gland. *Int J Dev Biol*. **55**, 745-755 (2011).
69. Adamson, T. W. *et al.* Assessment of carprofen and buprenorphine on recovery of mice after surgical removal of the mammary fat pad. *J Am Assoc Lab Anim Sci*. **49**, 610-616 (2010).
70. Doornebal, C. W. *et al.* Morphine does not facilitate breast cancer progression in two preclinical mouse models for human invasive lobular and HER2(+) breast cancer. *Pain*. **156**, 1424-1432 (2015).
71. Fischer, A. H., Jacobson, K. A., Rose, J., & Zeller, R. Paraffin embedding tissue samples for sectioning. *CSH Protoc*. **2008** (2008).
72. Cardiff, R. D., Miller, C. H., & Munn, R. J. Manual hematoxylin and eosin staining of mouse tissue sections. *Cold Spring Harb Protoc*. **2014**, 655-658 (2014).
73. Maller, O. *et al.* Collagen architecture in pregnancy-induced protection from breast cancer. *J Cell Sci*. **126**, 4108-4110 (2013).
74. Martinson, H. A., Jindal, S., Durand-Rougely, C., Borges, V. F., & Schedin, P. Wound healing-like immune program facilitates postpartum mammary gland involution and tumor progression. *Int J Cancer*. (2014).
75. Day, C. P. *et al.* "Glowing head" mice: a genetic tool enabling reliable preclinical image-based evaluation of cancers in immunocompetent allografts. *PLoS One*. **9**, e109956 (2014).

76. Schafer, M., & Werner, S. Cancer as an overhealing wound: an old hypothesis revisited. *Nat Rev Mol Cell Biol.* **9**, 628-638 (2008).
77. Kuraishy, A., Karin, M., & Grivennikov, S. I. Tumor promotion via injury- and death-induced inflammation. *Immunity.* **35**, 467-477 (2011).
78. Herreros-Villanueva, M., Hijona, E., Cosme, A., & Bujanda, L. Mouse models of pancreatic cancer. *World J Gastroenterol.* **18**, 1286-1294 (2012).
79. Johnson, R. L., & Fleet, J. C. Animal models of colorectal cancer. *Cancer Metastasis Rev.* **32**, 39-61 (2013).